Tilted view reconstruction in optical microscopy

Three-dimensional reconstruction of *Drosophila melanogaster* embryo nuclei

Peter J. Shaw,* David A. Agard,‡ Yasushi Hiraoka,‡ and John W. Sedat‡

*Department of Cell Biology, John Innes Institute, and AFRC Institute of Plant Science Research, Colney Lane, Norwich, NR4 7UH United Kingdom; ‡Department of Biochemistry and Biophysics, University of California Medical School, San Francisco, California 94143-0054, and The Howard Hughes Medical Institute, Structural Biology Unit, University of California, San Francisco, California 94143-0054

ABSTRACT The resolution along the optical axis (z) is much less than the in-plane resolution in any current optical microscope, conventional or otherwise. We have used mutually tilted, through-focal section views of the same object to provide a solution to this problem. A tilting specimen stage was constructed for an optical microscope, which with the use of a coverslip-free water immersion lens, allowed the collection of data sets from intact *Drosophila melanogaster* embryos at viewing directions up to 90° apart. We have devised an image processing scheme to determine the relative tilt, translation, and sampling parameters of the different data sets. This involves the use of a modified phase cross-correlation function, which produces a very sharp maximum. Finally the data sets are merged using figure-of-merit and local area scaling techniques borrowed from x-ray protein crystallography.

We demonstrate the application of this technique to data sets from a metaphase plate in an embryo of *Drosophila melanogaster*. As expected, the merged reconstruction combined the highest resolution available in the individual data sets. As estimated from the Fourier transform, the final resolution is 0.25 μm in x and y and 0.4 μm in z.

In the final reconstruction all ten chromosome arms can be easily delineated; this was not possible in the individual data sets. Within many of the arms the two individual chromatids can be seen. In some cases the chromatids are wrapped around each other helically, in others they lie alongside each other in a parallel arrangement.

INTRODUCTION

The recent availability of a wide variety of specific fluorescent probes, such as fluorescently labeled DNA, monoclonal antibodies, and specific organic dyes for chromatin and ions such as calcium, has led to a renaissance in optical microscopy as a tool in cell and molecular biology. Biological material can be surveyed quickly and in something close to its native state. Cellular structures are complicated three-dimensional objects, however, and this has given rise to methods for determining three-dimensional structure using optical microscopy. While a high numerical aperture objective lens can give resolution limits of a fraction of a micron in the focal plane, a major limitation of conventional optical microscopy as a tool for three-dimensional structure analysis is the lack of resolution in the direction of the optical axis (z) as compared to the in-plane resolution.

The reason is inherent in the optics of a conventional microscope. Each point in the object gives rise to a blurred counterpart in the image known as the point spread function (PSF). The central section of the PSF is the familiar Airy disc; in three dimensions the PSF has a complicated conical form, diverging on either side of the focal plane (see, for example, references 6 and 10). For many purposes the PSF is more easily understood in terms of its Fourier transform, which is called the contrast transfer function (CTF). The Fourier transform of the image then consists of the Fourier transform of the object multiplied by the CTF. In the three-dimensional CTF the lack of resolution in z is apparent as a missing cone of information (1).

Several workers have sought to alleviate this problem by computer imaging processing of the three-dimensional optical section stack (1–3, 5, 6, 16). Although these methods improve the clarity and ease of interpretation of the images, it is not clear that they are capable of restoring the missing data and thus truly increasing the resolution in z. Concurrently, an alternative to the conventional optical microscope, the confocal scanning microscope, has been developed, and has recently been applied to imaging biological structures by immunofluorescence (14–16). This type of microscope shows great promise in increasing the overall resolution, but the resolution available in the z direction is still much less than the in-plane resolution. We describe in this paper the use of an approach familiar in the fields of x-ray crystallography and electron microscopy, that of tilting the specimen to measure explicitly the data missing in images measured from a single direction. Although small amounts of specimen tilt have been used in optical microscopy to give stereo views (see, e.g., 13), no one, to our knowledge, has previously attempted to use tilted optical data to reconstruct a three-dimensional image.

0006-3495/89/01/101/10 $2.00

This approach has been prompted by our interest in the detailed arrangement of diploid chromosomes in *Drosophila melanogaster* embryos. These specimens are close to the resolution limit of a conventional optical microscope; typically the whole mitotic figure is only 4–5 μm across and individual chromosomes are less than 0.4 μm in diameter. Thus reliably determining three-dimensional structures of these specimens poses a challenging problem in optical microscopy.

MATERIALS AND METHODS

Tilt stage construction

The tilt stage was constructed, after several earlier versions, with the aim of being able to tilt the specimen through large angles eucentrically to a precision of better than 1 μm. It was designed so that any desired portion of a large biological sample, for example, a single diploid nucleus (4–5 μm in diameter) in an intact *Drosophila* embryo, could be moved to the center of rotation. A photograph of the tilt stage mounted on the Zeiss Axiomat microscope is shown in Fig. 1. The stage is based on a precision, duplex 40-mm bearing. The tilt rotation is powered by a DC motor with an attached tachometer and an encoder giving an effective 20,000 lines/revolution (Aerotech Inc., Pittsburgh, PA). Computer control of the motor is through a Z8 microcomputer and is driven as a menu option in the data collection program in a very similar way to the computer focus control. The bearing assembly is mounted on a crossed-roller bearing translation stage, which gives ~50 mm of travel with <0.5 μm runout error, in the direction of the tilt axis (part No. 435A-2; Newport Corp., Fountain Valley, CA). To the end of the tilt shaft is attached a small *x-y* translation stage, each axis being driven by a miniature gear motor (part No. M9115 L61-208; Portescap, La Chaux-de-Fonds, Switzerland), powered by a modified Zeiss Axiomat *x-y* controller. This translation stage then carries the mounting plate for the specimen capillary, which is clamped into a V-shaped groove carefully aligned parallel to the tilt axis. The entire assembly is clamped with heavy mounting bolts to the Axiomat chassis. These mounting bolts have micrometer screws which allow fine adjustment of the stage centering.

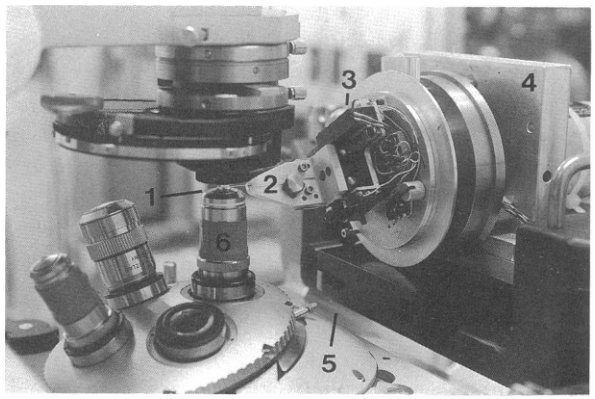

FIGURE 1 Tilt specimen holder on axiomat microscope. (1) Specimen capillary tube; (2) capillary mounting plate; (3) specimen *x-y* translation stage; (4) tilt bearing; (5) tilt axis translation stage; (6) microscope objective lens.

For centering of the stage, a fine needle is mounted in place of the specimen capillary and brought to the tilt axis by adjustment in the *x-y* translation until the tip remains in the same position as it is tilted. It is then brought to the center of the field of view with the stage centering screws. At this stage the alignment of the tilt axis with the CCD camera *x* axis is checked by offsetting the needle to one side and tilting through 180°. If the axis is aligned this should result in a translation purely in the *y* direction.

It was appreciated after this stage was built that there are several places where changes could be made to reduce expense and complexity. First, the bearing might be a precision "V" groove with a ground shaft. Second, for some purposes the tilt motor system might be replaced by manual control (with a simple angle readout). Finally, if motor control of the tilt is necessary, a microstepping motor system (for example Compumotors, Petaluma, CA), which gives smooth movement and is easy to interface, should be considered.

Data collection

Drosophila melanogaster embryos were fixed with 3.7% formaldehyde in heptane/buffer A (15 mM Pipes, pH 7.0, 20 mM NaCl, 0.5 mM EGTA, 2 mM EDTA, 0.5 mM spermidine, 0.2 mM spermine, 0.1% 2-mercaptoethanol). The chorion and vitelline membrane were removed as described previously (11). The embryos were stained with 0.1 μg/ml DAPI and examined on a Zeiss Universal epifluorescence microscope to determine their stage of development. The selected embryo was attached to a glass capillary tube by gently touching it with the tube, which had been pre-treated with 0.02% poly-L-lysine. The capillary tube with the specimen attached was then mounted on the Axiomat tilt stage. For the capillary tubes we used thin-walled 0.3-mm quartz glass tubes glued into thicker (2 mm) glass tubes for most of their length for strength and stability. Before data collection, the specimen was moved to the plane of the stage tilt axis, by adjusting the focus and specimen height until the specimen remained centered in the field of view as it was tilted (i.e., was located at the eucentric axis of the stage).

Data sets were collected using a water immersion objective lens (Zeiss, 63×, NA 1.2). Buffer A was used as the immersion medium to maintain the specimen preservation. (The 2-mercaptoethanol in buffer A also acted as an anti-fade agent, presumably by scavenging free oxygen in the medium.) First a suitable nucleus was selected for measurement, and the total range of tilt that could be achieved without obstruction was determined. In favorable cases, −45° to +45° was possible. Then a series of data stacks was measured, the tilt angle being set to the required value for each stack under computer control. The automated data collection using a CCD (charge coupled device) camera has been described before (8). The in-plane sampling used was 0.06 μm, and image planes 512 × 512 were measured. The focus step between sections was generally 0.2 or 0.25 μm, and an embryonic mitotic plate nucleus would typically require about 30 optical sections. The number of tilted data sets that could be collected was determined essentially by the specimen fading. Although in one case it was possible to measure five data sets, the data were not good, and more usually two or three data sets were collected.

Data processing

More detailed descriptions of the background to optical sectioning microscopy and the computer processing entailed are given in reviews (1, 2). The data processing scheme is shown in diagrammatic form in Fig. 2. The overall strategy was first to select and mask the regions of interest from the data stacks. Next the relative translation, orientation, and sampling parameters between the tilted data sets were determined using the cross-correlation procedure described below. Then each data

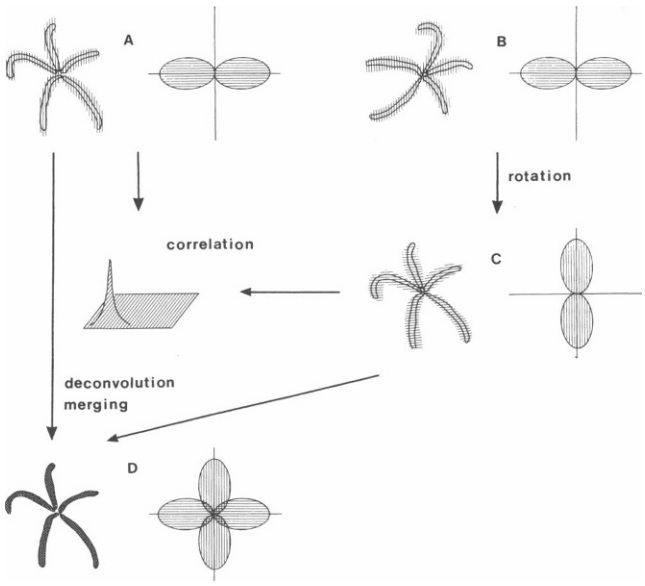

FIGURE 2 Diagrammatic representation of the image processing scheme, showing the interrelationship of images and their Fourier transforms. At each stage (*A–D*) a pair of figures is shown: that on the left representing a three-dimensional image, that on the right its three-dimensional Fourier transform. (*A*) An object and its transform as viewed from the first direction. (*B*) The same object physically rotated and viewed from a second direction. (*C*) The view shown in *B* is resampled by computation in a rotated coordinate frame (i.e., it is effectively rotated back in the computer to be an equivalent view to *A*). (*D*) A three-dimensional cross-correlation function is calculated from the original view (*A*) and the other view rotated (*C*), and the position of the peak on the resulting correlation map used to align the two data sets. Finally the data sets are individually sharpened by deconvolution and merged.

stack was individually deblurred so as to bring back the high spatial frequency image content to its correct level as judged by the measured CTF. Finally the tilted, deblurred data stacks were merged after applying the initially determined parameters.

All data processing was carried out on a VAX 8650 computer, using programs written in VAX Fortran. Images were displayed on a DeAnza 6400 image processor (Gould Inc., San Jose, CA). Before reconstruction was attempted, each data set was examined carefully for systematic errors. In some data sets a systematic small drift, primarily in the direction parallel to the tilt axis, was detected. This was typically less than one pixel between successive sections, but could accumulate to more than 10 pixels over the whole stack. It was therefore corrected; the displacement between successive sections was calculated from the peak position of their two-dimensional cross-correlation function (4):

> For two data planes denoted by $f_1(x)$ and $f_2(x)$ we denote their Fourier transforms by $F_1(S)$ and $F_2(S)$. Then the Fourier transform of the cross-correlation is given by:
>
> $$X(S) = F_1(S)\, F_2(S)^*,$$

where (F2(S)* denotes the complex conjugate. The peak position of the correlation maximum was determined by fitting a quadratic function to the nine points surrounding the highest point in the function, and the calculated offsets were used to resample the data planes by interpolation.

Next the area of interest in the data set was masked from the surroundings and the image was trimmed to exclude unwanted areas. At this stage the sections were also normalized to the same total integrated intensity to correct for fading and any changes in intensity of the light source.

To determine the relative origins of the data sets a modified cross-correlation function was calculated, via three-dimensional Fourier transforms:

> Using the same nomenclature as above, but now letting $f_1(x)$ represent the first three-dimensional image stack, and $f_1(x)$ the second stack rotated to the same orientation as $f_2(x)$, the Fourier transform of the modified cross correlation is defined by
>
> $$X(S) = [F_1(S)(F_2(S)^*]/[(|F_1| + S_1)(|F_2| + S_2)].$$

This correlation function effectively replaces each Fourier term by its phase, giving a very much sharper correlation peak. The terms S_1 and S_2 are constants chosen so as to limit the contribution of small amplitude coefficients which are primarily noise, and are analogous to similar factors in a Wiener filter (see, e.g., reference 6). The peak of the correlation map was determined by fitting a quadratic polynomial to the points surrounding the maximum. This correlation procedure was then embedded into a program which searched for the best values for relative tilt angles and relative pixel spacings by finding the maximum correlation peak height (again by quadratic interpolation) with respect to the parameter being refined.

Before merging the data sets, each was individually corrected for the effects of the three-dimensional contrast transfer function. For this deconvolution the point spread function for the objective lens was measured using fluorescent beads. Its three-dimensional Fourier transform was then calculated and averaged in bands of constant radius to give a radially symmetric CTF. Various algorithms were tried for the deconvolution process: a simple, linear Wiener-type filter; a full three-dimensional iterative constrained method analogous to that described by Agard and colleages (1, 2); and a modification of a recently described entropy-based method (8). The deblurred image shown in the present paper were produced by the iterative, constrained method.

Finally the data sets were merged using the determined alignment parameters. First the three-dimensional Fourier transform of each data set was calculated. Then the transforms were combined point by point, treating the amplitude and phase data separately as is common in x-ray crystallography. (The rationale for this is that the image degradation due to the objective CTF is primarily an amplitude filter; the phases should to a first approximation be unaffected, although the reliability of their measurement will of course depend on the associated amplitudes.) For each point in the Fourier transforms the combined phase was calculated as the phase of the vector sum of the individual values. Each combined value was weighted by a figure of merit calculated as the cosine of the minimum phase discrepancy between the individual phases and the combined phase. For the amplitudes, a local area scaling approach was used. Amplitude scale factors were calculated in volumes of Fourier space. Then a weighted mean amplitude was calculated:

$$F_{bar} = (F_1{}^*F_{1scale} + F_2{}^*F_{2scale})/(F_1 + F_2),$$

> where F_1 and F_2 are the original amplitudes and F_{1scale} and F_{2scale} are the amplitudes scaled by the local scaling factors, where the region of smaller mean amplitude is scaled up to the larger.

The final reconstruction was then calculated by inverse Fourier transformation.

For examining the reconstructions and intermediate results we found it extremely helpful to calculate stereo projections of the entire three-dimensional image, as well as examining individual sections. For the

stereo projection an efficient algorithm was devised which allowed computation of various projected views quickly. From a data set containing a series of views about a single axis it was possible to produce the effect of rocking the structure back and forth by successively displaying the series.

RESULTS

A central concern of this laboratory is the determination of the detailed three-dimensional arrangements of diploid chromosomes in *Drosophila* throughout the cell cycle. The small size of these chromosomes (the complete metaphase plate may be only 4–5 μm in its largest dimension) makes this a very difficult problem. It has become apparent that it is often not possible to trace these chromosomes unambiguously in an optical section data stack collected from a single viewing direction, even after deblurring of the data. The reason is primarily lack of resolution in the direction of the optical axis. We therefore attempted to resolve these difficulties by devising a method of tilting the specimens through large angles and collecting additional data sets. Initially the aim was to use the additional data to resolve the ambiguities in the zero tilt data sets, however it became apparent that a more rigorous and elegant approach would be to combine all the data into a single reconstruction, and we therefore developed the technique described here.

The data shown in this paper are from a metaphase plate from an intact stage 12 *Drosophila melanogaster*

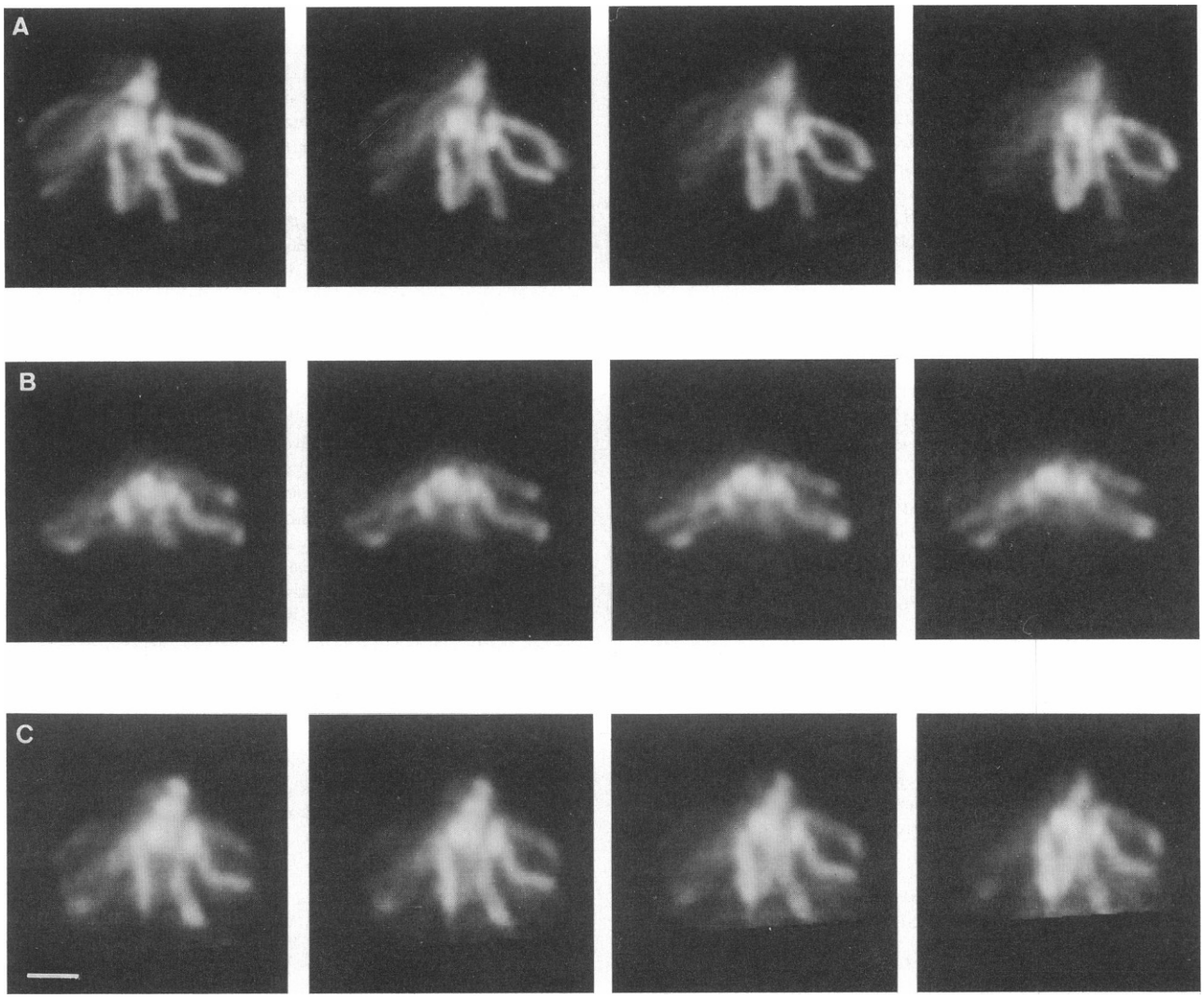

FIGURE 3 Sample sections from the unprocessed data stacks. (*A*) Consecutive sections from the data stack at 0° tilt angle. (*B*) Consecutive sections from the data stack at 45° tilt angle. (*C*) Consecutive sections from the data stack at 45° tilt angle rotated by computation to 0° tilt. Bar, 2 μm.

embryo. High quality data were obtained at 0° and +45° specimen tilt using the CCD camera system. A selection of the unprocessed optical sections from each data set is shown in Fig. 3. A third data set at −45° was also measured; however, fading of the fluorescence resulted in poorer quality data for this view, and the data set was not used in the reconstruction. Because of the complexity of this three-dimensional object, the initial sections look, as expected, very different (Fig. 3, *A* and *B*) but when the data set at 45° is resampled at 0° by interpolation it looks very similar to the true 0° set, although affected differently by the CTF (Fig. 3 *C*).

The fundamental problem to be solved before the data sets can be combined is one of alignment; the data sets must all be rotated and translated to a common origin and coordinate system. A standard approach to this problem, which has recently begun to be used extensively in high resolution electron microscopy (see, e.g., reference 12), is to calculate the cross-correlation function (5). A straightforward cross-correlation between the zero tilt and resampled 45° data sets showed a clear, but very broad, maximum; it was not possible to determine its peak position with enough precision for it to be useful. The reason that this type of correlation function has such a broad peak is that it is dominated by very low frequency terms which typically have a very much greater amplitude than the high frequency terms. It is these latter terms that represent the detail in the images that we wish to recover. We therefore calculated what is effectively a cross-correlation function using only the phases of the data. In order to prevent noise from dominating this correlation map a noise damping factor, analogous to the noise-to-signal term in a standard Wiener filter, was added. The modified phase cross-correlation showed a very much sharper and more precisely defined peak. Fig. 4 shows a comparison of the conventional and phase cross-correlation map for these two data sets. The peak position of the modified cross-correlation can clearly be located to within a fraction of a pixel.

It soon became clear from comparing tilted and untilted data sets in detail that the interplanar spacing had been overestimated. However the phase cross-correlation map shows such a sharp peak and high peak-to-background ratio that it is possible to use this function also to refine the correct geometrical parameters between the data sets. The correct value for the spacing was therefore determined by systematically varying it and finding the value that maximized the height of the correlation peak. The correlation showed a clear maximum at 0.16 μm (compared to 0.2 μm actual movement of the objective) (Fig. 5). This discrepancy is confirmed by similar results for several other tilted data sets (Table 1), and we believe it is due to different refractive indices in the immersion medium and specimen (see Discussion).

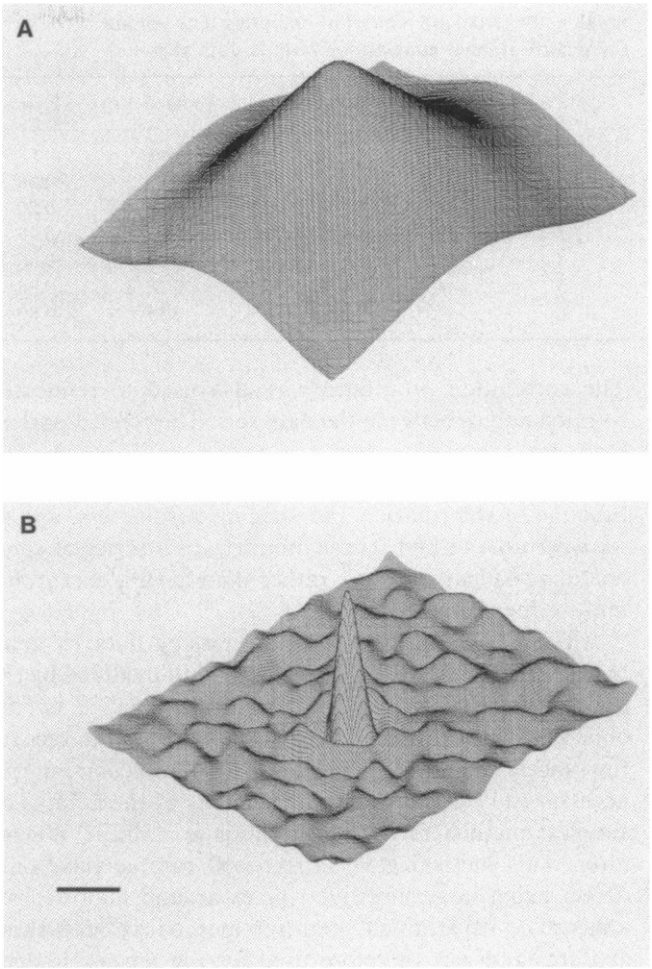

FIGURE 4 Representations of planes from the three-dimensional correlation maps containing the maximum correlation peak. (*A*) Conventional cross-correlation map. (*B*) Phase/Wiener cross-correlation map. In *A*, the peak extends effectively across the whole plane, whereas in *B*, it is very much more precisely defined. Bar, 2 μm.

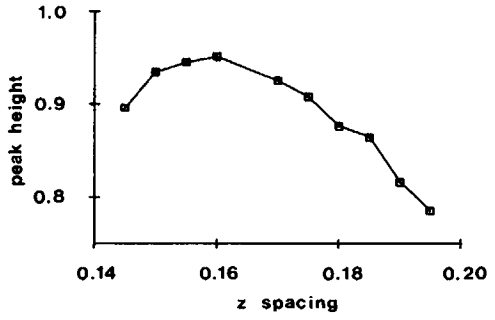

FIGURE 5 Graph of correlation peak height with respect to *z*-spacing assumed for the calculations. The physical movement of the objective lens between sections was 0.2 μm, whereas the correlation function shows a clear peak at 0.16 μm. This discrepancy is probably due to an "apparent" depth effect.

TABLE 1 Physical movement of objective lens versus refined interplanar spacing for various data sets

Data sets	Angle	Movement	Refined Δz	Ratio
		μm	μm	
1	+30°	0.50	0.43	0.86
2	−20°	0.50	0.40	0.80
3	+25°	0.35	0.27	0.77
4	+45°	0.35	0.30	0.86
5	−45°	0.35	0.28	0.80
6	+45°	0.20	0.16	0.80

The correlation procedure was also used to refine the rotation angles between the data sets. The refined parameters for these data sets are shown in Table 2. The correlation peak height is a very smooth and well behaved function of the rotation and spacing parameters, and so we were able to find its maximum with a series of short one-dimensional searches, rather than having to search a multi-dimensional space.

Although we can measure the missing data by combining tilted data stacks, the data are still modified by the great fall-off with respect to resolution implied by the objective lens CTF (see Fig. 6 *A*). As we wish to recover the highest resolution image detail at its full contrast, it is necessary to compensate for the effects of the CTF. The simplest method for this calculation is a linear Wiener filter. This method gave fairly good results, their only defect being large negative ripples around high density areas. The constrained, iterative method avoided these artifacts and was therefore used for the reconstructions shown in this paper. We found it was important to use the measured CTF in the deconvolution, rather than any theoretical, calculated CTF (for example, see references 1 and 7). The radial fall-off given by the theoretical calculations is considerably greater than shown in practical measurements.

Some sections from the final reconstruction are shown in Fig. 7. The merged image was very similar to the zero tilt deconvoluted stack when viewed as x-y sections, however, the increase in z resolution produced by the inclusion of the tilted data was clear when equivalent x-z sections were compared (see Fig. 8). There is much less smearing in z in the combined reconstruction, features are more clearly defined in extent, and generally the x-z sections have a similar overall character to the x-y sections. As an indication of the resolution, a radial projection of the Fourier transform amplitudes of the reconstruction is shown in Fig. 6 *B*. As judged by significant power in the transform, the resolution extends to 0.25 μm in x and y and ~0.4 μm in z at $x,y = 0$ (the z resolution is better at higher x,y spatial frequencies).

TABLE 2 Initial versus refined orientation, translation, and sampling parameters for illustrated data sets

	R_x	R_y	R_z	T_x	T_y	T_z	Δx*	Δy*	Δz
Initial	45.0°	0.0°	0.0°	0.0	0.0	0.0	0.06	0.06	0.20
Refined	44.0°	2.3°	−0.2°	−13.3	−5.1	−0.28	0.06	0.06	0.16

*Not refined.

R_x, R_y, R_z rotations around x, y, z axes, respectively. T_x, T_y, T_z translations in x, y, z, respectively. Δx, Δy, Δz pixel spacing in x, y, z, respectively.

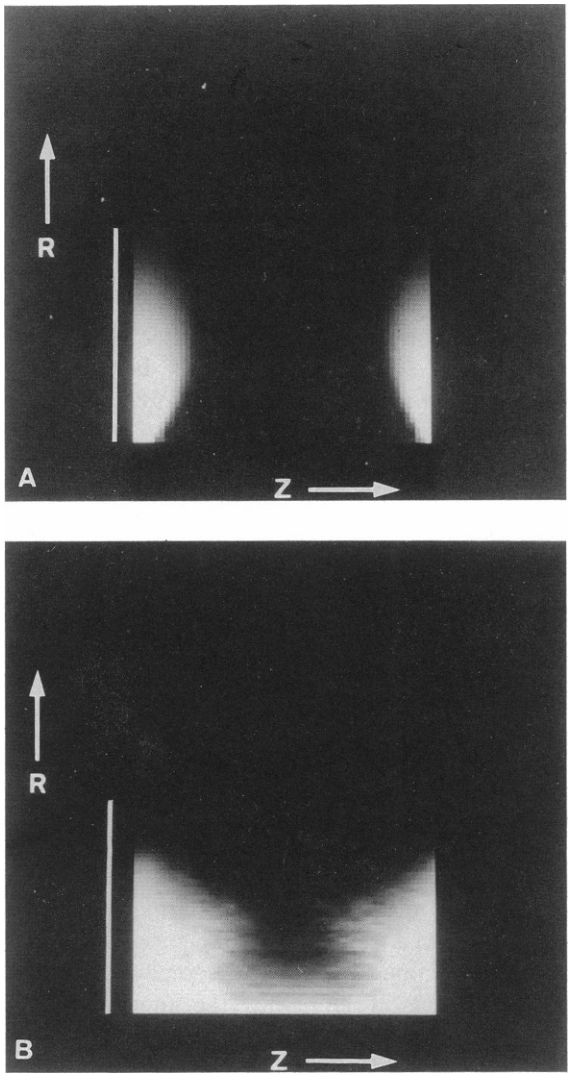

FIGURE 6 (*A*) Radial projections (i.e., averaged in bands of constant radius) of the measured contrast transfer function for the 63× water immersion lens (NA 1.2). (*B*) Radial projection of the three-dimensional Fourier transform of the merged reconstitution. In each case the sampling has been interpolated so as to give a true, isotropic representation of the projections. The radial direction (i.e., perpendicular to the optical axis) is shown vertical and Z (i.e., parallel to the optical axis) horizontal. R is given by $(X^2 + Y^2)^{1/2}$, where X, Y, and Z are Fourier space components (in units of reciprocal microns). Bar, 1/0.24 μm^{-1}. Note that the actual resolution shown in *B* is much more nearly isotropic than that shown by the CTF in *A*.

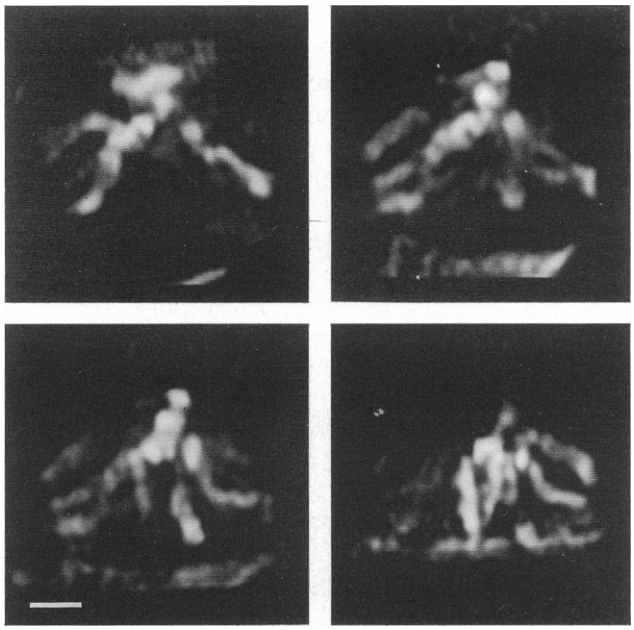

FIGURE 7 Some sections from the final merged reconstruction. In many cases the individual chromatids are visible within the chromosomes arms. Bar, 2 μm.

Stereo projections at 0° and 45° of the individual and merged data sets are shown in Fig. 9. It is clear that the merged data set combines the best resolution available in each individual data set.

All ten chromosome arms can now clearly be seen and can be followed without difficulty to a central region where the centromeres are clustered. When combined with rotational rocking of stereo views, the course of the chromosomes can be followed even through this complicated region. In at least five of the arms, substructure corresponding to the individual chromatids can be seen (also see Fig. 7). In places the two chromatids are wound around each other in helical structures, in others they appear to by lying more parallel to each other. Reconstructions such as these are in the process of interpretation and modeling in this laboratory, and the full results of their interpretation will be presented in a later paper.

DISCUSSION

We have shown that it is practicable to collect optical section stacks of the same object tilted through large angles, and that these data sets show differences in their degradation by the objective contrast transfer function. Furthermore we have shown that it is possible to determine the relative tilt, translation, and sampling parameters directly from the images themselves. Finally we have devised a way to combine the data sets in a way that

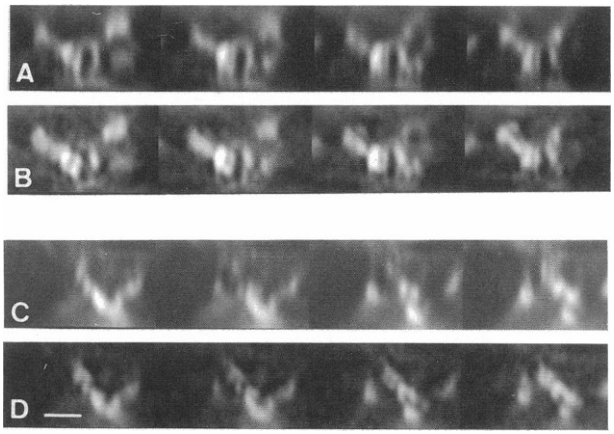

FIGURE 8 Comparison of equivalent x-z sections from merged reconstruction (B, D) and deblurred, 0° tilt data set (A, C). Bar, 2 μm.

effectively gives the best resolution available in each individual data set. Thus in principle diffraction limited resolution could be obtained equally in all three dimensions. In practice we have obtained a Fourier transform resolution of 0.25 μm in x and y and 0.4 μm in z. (By the Rayleigh resolution criterion, this would distinguish three-dimensional gaussian functions separated by 0.15 μm in x and y and 0.24 μm in z.) Because of the shape of the CTF the effective resolution in z is better than these values. The agreement between the tilted data stacks provides convincing evidence that such optical section stacks give a faithful representation of the three-dimensional structure of the specimen, to the limits imposed by the CTF of the objective lens.

In such a procedure it is important to estimate the accuracy with which the data sets must be aligned. As a guide to this, we shall estimate the error in any of the parameters that would give a maximum offset between the tilted images of one-quarter the wavelength of the fluorescent radiation (i.e., half the maximum resolution expected or 0.12 μm for staining with DAPI). Relating this to the data sets described in this paper, this corresponds to two pixels in x and y and 0.75 pixels in z. The precision with which the correlation peak can be determined is clearly much better than this. For angular parameters, given an object of approximate size 7 by 7 by 7 μm, an error of 0.12 μm at the periphery of the object corresponds to an angular error of ~2°. In our refinement, the angular parameters refined close to the values set on the tilt stage (see Table 2); however, there were slight differences which we attribute to slight missetting of the rotation axis with respect to the measurement coordinate system (defined by the optic axis and the position of the CCD camera). Thus it seems necessary to refine the orientation angles even for a small object such as this. Larger objects would need more accurate values for the

rotation angles, but the refinement should be correspondingly more sensitive to the rotation angles. As an additional test we calculated the peak height as a function of tilt angle from a rotation of 25° to 65° (see Fig. 10). This showed a clear well defined peak. Thus it should be possible to determine the setting angle substantially from the data itself, even if known only to within 20°. Finally, the spacing in z (relative to that in x and y) must be correct to an accuracy of 0.12/3.5, or ~3.5%. Again, we were able to refine this value by the correlation procedure.

The difference between the physical movement in the objective plane and the actual change in focal plane was unexpected (see Table 1). We are confident it is a real effect, having checked the accuracy of the focus movement carefully. It can be rationalized as being due to the difference in refractive index of the specimen at the focal plane (in this case chromatin) and at the objective (water or buffer A). A simple calculation shows that the ratio of physical to optical step sizes is equal to the ratio of refractive indices. Since we have observed a step size ~15% less than the focus movement, this implies a refractive index at the specimen of ~1.6. This does not seem unreasonable. Interestingly, it is close to the refrac-

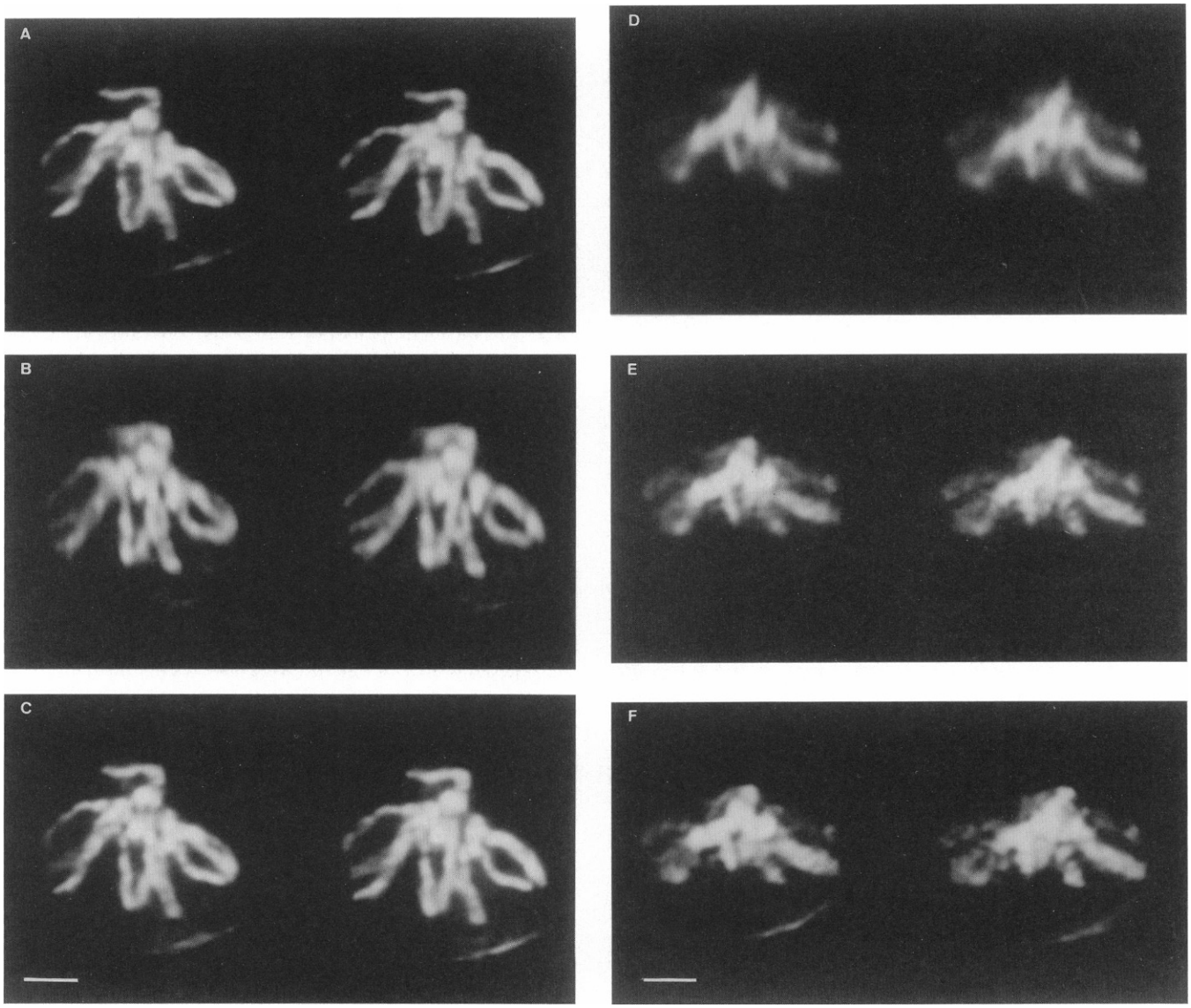

FIGURE 9 Stereo projections of the deblurred 0° and 45° tilt data sets, and of the merged reconstruction. (*A*) 0° tilt data set projected at 0°. (*B*) 45° tilt data set projected at 0°. (*C*) merged data set projected at 0°. (*D*) 0° tilt data set projected at 45°. (*E*) 45° tilt data set projected at 45°. (*F*) merged data set projected at 45°. The individual data sets, although clear when projected along the direction in which they were collected, are blurred when projected in the other direction. The merged data set effectively combines the best view of each data set.

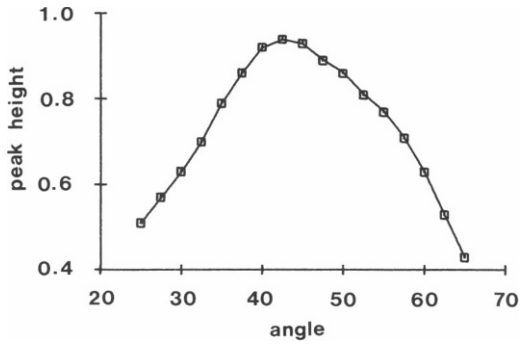

FIGURE 10 Graph of peak height with respect to angle, showing that the correlation approach can determine the rotation angle with considerable precision, even if the starting value is known only very approximately.

tive index of immersion oil, and so this focus effect may not be important when using oil immersion lenses.

The scheme we have used to combine the data sets is somewhat ad hoc. The rationale for the figure of merit weighting, borrowed from x-ray crystallography, is to preserve unchanged those Fourier components where the phases agree well, or where the component from one data set is much stronger in amplitude, but to weight down those components which disagree in phase but have similar amplitudes. In practice the weighting scheme does not have a large effect on the final reconstruction. A more rigorous method of combination would be to modify the constained, iterative deconvolution method so as to calculate the corrections to the trial solution by examining its agreement with all the tilted data sets simultaneously. We have not so far attempted this. It should also be possible to determine the focal plane dependence of the three-dimensional CTF from the images themselves given two or more mutually tilted data sets. We have not done so yet. In practice the local area amplitude scaling we used, where in each case the area of smaller mean amplitude is scaled up to the larger, should remove any residual CTF dependent discrepancies. However it would be interesting to discover how well the CTF determined from measurements on small beads agreed with that displayed by a large scale object.

The fact that it is possible to refine the orientation parameters from the data sets themselves substantially relaxes the requirements for the tilt stage. The most important consideration is ease of use rather than physical tolerance. If it is only necessary to be able to rotate the specimen and know the relative tilt to within 10° or 20°, a very simple method for holding and rotating the capillary will suffice. However this would entail a substantial penalty in terms of ease of tracking the specimen during rotation. For many specimens it is clearly necessary to be able to move the desired portion to the eucentric axis in order to be certain that one and the same part of the specimen is examined in the different directions. In this case it is necessary to have translational motion of the specimen holder with respect to the rotation axis. In our experience, to make such a system usable, it is necessary to have this translation movement motor-driven. As regards the rotation itself, although stability is of crucial importance, accurate positional setting is not. The motor drive could thus probably be dispensed with for the rotation. It might even be possible to dispense with a tilt stage altogether for some specimens and obtain two views using a microscopic mirror system similar to that described by Boocock et al. (4).

There is clearly much more information available in a set of tilted images as compared to a single optical section stack. It may not be always be necessary to combine the tilted data sets into a single reconstruction to make effective use of this information in interpretation. With this in mind, a new computer modeling program has been written in this laboratory which allows modeling from two or more tilted views simultaneously. If, however, a single reconstruction is required, the method we have presented has the potential of yielding near isotropic resolution in three dimensions. The limitations are practical. First, the maximum angle to which the specimen can be tilted depends on the nature of the specimen itself. (In the case of the *Drosophila* embryos, other parts of the embryo begin to obscure the portion of interest past + and −45°.) Second, the maximum tilt angle is limited by the working distance of the objective lens—current, high numerical aperture lenses have very small working distances. Finally, we should stress that although we have used conventional fluorescence optics, the technique described is equally applicable to any other imaging mode, notably to data from confocal scanning fluorescence microscopy. The better the resolution in the starting data, the better correspondingly the resolution in the final reconstruction.

There are many problems in cell biology where accurate three-dimensional data is of crucial importance. Apart from the studies of nuclear architecture in which these laboratories are engaged, areas such as cytoskeleton arrangements and rearrangements, cell surface receptors, and time-resolved determinations of the distribution of calcium and other ions are clearly three-dimensional problems which require three-dimensional solutions. In our experience there are situations in which data collected from a single view cannot provide enough information, and as increasingly accurate determinations of the cellular apparatus are sought many other such situations will arise in diverse areas of cell biology. We have presented a method which will allow the many advantages of optical microscopy to be extended to nearly isotropic three-dimensional resolution.

This work was supported by the Agricultural and Food Research Council via a grant-in-aid to the John Innes Institute (P. J. Shaw). Support was also received from the Gatsby Foundation (P. J. Shaw). Y. Hiraoka was supported by Damon Runyon-Walter Winchell Cancer Research Fund Fellowship DRG903. J. W. Sedat and D. A. Agard are both Howard Hughes Investigators. D. A. Agard is also a National Science Foundation Presidential Young Investigator. In addition, this work was supported by grants from the National Institutes of Health to J. W. Sedat (GM-25101) and to D. A. Agard (GM-31627).

Received for publication 13 May 1988 and in final form 15 September 1988.

REFERENCES

1. Agard, D. A. 1984. Optical sectioning microscopy: cellular architecture in three dimensions. *Annu. Rev. Biophys. Bioeng.* 13:191–219.
2. Agard, D. A., Y. Hiraoka, P. Shaw, and J. W. Sedat. 1988. Fluorescence microscopy in 3-dimensions. *Methods Cell Biol.* In press.
3. Agard, D. A., and J. W. Sedat. 1983. Three-dimensional architecture of a polytene nucleus. *Nature (Lond.).* 302:676–681.
4. Boocock, C. A., A. F. Brown, and G. A. Dunn. 1984. A simple chamber for observing microscopic specimens in both top and side views. *J. Microsc.* 137:29–34.
5. Bracewell, R. N. 1978. The Fourier Transform and its Applications. McGraw-Hill, Kogakusha.
6. Castleman, K. R. 1979. Digital Image Processing. Prentice-Hall, Inc., Englewood Clifts, NJ.
7. Erhardt, A., G. Zinser, D. Komitowski, and J. Bille. 1985. Reconstructing 3-D light-microscopic images by digital image processing. *Appl. Opt.* 24:194.
8. Gonsalves, R. A., and H. M. Kou. 1987. Entropy-based algorithm for reducing artifacts in image restoration. *Opt. Eng.* 26:617–622.
9. Hiraoka, Y., J. W. Sedat, and D. A. Agard. 1988. The use of a charge-coupled device for quantitative optical microscopy of biological structures. *Science (Wash. DC).* 238:36–41.
10. Inoue, S. 1986. Video Microscopy. Plenum Publishing Corp., New York.
11. Mitchison, T. J., and J. W. Sedat. 1983. Localization of antigenic determinants in whole *Drosophila* embryos. *Dev. Biol.* 99:261–264.
12. Saxton, W. O., and J. Frank. 1977. Motif detection in quantum noise-limited electron micrographs by cross-correlation. *Ultramicrosc.* 2:219–227.
13. Skaer, R. J., and S. Whytock. 1975. Interpretation of the three-dimensional structure of living nuclei by specimen tilt. *J. Cell Sci.* 19:1–10.
14. van der Voort, H. T. M., G. J. Brakenhoff, J. A. C. Valkenburg, and N. Nanninga. 1985. Design and use of a computer controlled confocal microscope for biological applications. *Scanning.* 7:66–78.
15. White, J. G., W. B. Amos, and M. Fordham. 1987. An evaluation of confocal versus conventional imaging of biological structures by fluorescence light microscopy. *J. Cell Biol.* 105:41–48.
16. Wijnaendts van Resandt, R. W., H. J. B. Marsman, R. Kaplan, J. Davoust, E. H. K. Stelzer, and R. Stricker. 1985. Optical fluorescence microscopy in three dimensions: microtomoscopy. *J. Microsc.* 138:29–34.